Mausam, (1992), **43**, 4, 365-370

550.34.013.4

Earthquake source parameter estimation using synthetic waveform modelling

R. S. DATTATRAYAM

India Meteorological Department, New Delhi

(*Received 7 May 1991*)

सार–संश्लिष्ट तरंगरूप मॉडलिंग का प्रयोग करते हुए हिमालय संघट्ट क्षेत्र में घटने वाले तीन भूपर्पटी घटनाओं के लिए भ्रंशतल सॉल्यूशन और उद्गमकेन्द्र प्राप्त की गई। तिब्बती पठार में अपने अधिकेन्द्रों के साथ दो भूपर्पटी घटनाओं ने पूर्व–पश्चिम ट्रेंडिंग टी–एक्स सहित सामान्य भ्रंश के बड़े घटक दर्शाते हैं। मेन बाउंडरी थ्रस्ट (MBT) के उत्तरी अधिकेन्द्र की तीसरी भूकंप की नोडल तल स्थानीय संरचना ट्रेंड से समानान्तर होते हुए विपरीत भ्रंश दिखाता है। ये तीनों भूपर्पटी भूकंप पन्द्रह कि. मी. से कम सतही शैलों (फोकल) केन्द्रीय गहराइयों में घटित होती है। इन घटनाओं के अनुमानित स्रोत प्राचल क्षेत्र की, सक्रिय विवर्तनिकाओं को ध्यान में रखते हुए चर्चा की गई है।

ABSTRACT. Fault plane solutions and focal depths for three crustal events occurring in the Himalayan collision zone have been obtained using synthetic waveform modelling. Two crustal events with their epicentres in the Tibetan plateau show large component of normal faulting with east-west trending *T*-axes. The third event with it's epicentre north of Main Boundary Thrust (MBT) shows reverse faulting with the nodal planes paralleling the local structural trend. All the three crustal events studied have occurred at shallow focal depths of less than 15 km. The inferred source parameters of these events are discussed in the light of active tectonics of the region.

Key words — Waveform modelling, Synthetic seismograms, Fault plane solution, Source parameters, Himalayan collision zone.

1. Introduction

The current tectonic activity in central Asia has largely been attributed to the continued collision between the Indian and Eurasian plates. The stresses accumulated as a result of continued collision are being released through earthquakes of varying magnitudes. Accurate focal depths and reliable fault plane solutions play an important role in elucidating the physics of earthquake mechanism.

While the first motion and surface wave data enable us to draw fairly accurate information on fault geometry, information on body waves, by virtue of their high frequency content, yield higher resolution and thus characterise the source more in detail. The body wave modelling techniques, in which synthetic waveforms are generated and compared with the observed seismograms, have become one of the most important tools of observational seismology (Helmberger and Budrick 1979). The technique essentially consists of comparing the observed seismograms with the synthetic waveforms generated using a known source model and crustal structure. Iterative techniques are employed to get a best fit between the observed and synthetic waveforms by varying either the source properties or the crustal structure keeping other parameters constant. The parameters that yield the best fit are then taken as representative of the source. This study is aimed at placing constraints on focal depths and fault plane solutions for three shallow earthquakes in the Himalayan collision zone by comparing the observed seismograms with the synthetics generated using the algorithm developed by Kroeger and Geller (1983).

2. Method of analysis

The hypocentral parameters of the events studied, as reported in the ISC bulletins, are listed in Table 1. The synthetic seismograms have been computed using a program developed by Kroeger and Geller (1983), which includes all reflections and conversions from an assumed crustal structure near the source. Schematically, the observed seismogram can be expressed as a convolution of the form :

$$U(t) = S(t) * NSS(t) * E(t) * RS(t) * I(t)$$

where, $U(t)$ is the seismogram, $S(t)$ is the far-field source time function, $NSS(t)$ is the term which contains the effects of the focal mechanism of the source and propagation through the earth structure near the source, $E(t)$ is the term which includes the effects of propagation from the source region to the receiver region. It incorporates the travel time from the base of the near source structure to the base of the near-receiver structure, whole earth geometrical spreading and anelastic attenuation effects, $RS(t)$ is the near-receiver structure term, and $I(t)$ is the response of the seismic instrument.

TABLE 1

Earthquakes analysed

Event No.	Date	Location		m_b	Depth (km)
		Lat. (°N)	Long. (°E)		
1	23 Jan 1982 (17 hr)	31.68	82.28	6.0	26.0
2	29 Jul 1980 (14 hr)	29.63	81.09	6.1	23.0
3	22 Feb 1980 (03 hr)	30.55	88.65	5.7	10.0

TABLE 2

Crustal structure used in the study

Event No.	*Vp* (km/sec)	*Vs** (km/sec)	Density (gm/cc)	Thickness (km)
1 and 3	2.7	1.56	2.0	2.0
	6.2	3.58	2.75	19.0
	6.9	3.98	2.92	39.0
	8.0	4.62	3.28	—
2	2.7	1.56	2.0	6.0
	6.2	3.58	2.75	8.0
	6.9	3.98	2.92	14.0
	8.0	4.62	3.28	—

* Vp/Vs is assumed to be 1.73

Stein and Wiens (1986) have studied in detail the effect of near source structure, frequency response of the instrument and source parameters on the synthetics generated. For the long period data, moderate changes in the near source structure do not alter the depth determinations much, as some of the additional small phases are filtered out by the instrument. In the continental region, the depth determination is rather robust with respect to the crustal structure. The crustal structure obtained by Kaila *et al.* (1968) has been adopted in this study with little modifications. The crustal structure assumed for each event varies depending on the epicentral distance from the thrust axis and is listed in Table 2.

While the short period instruments resolve higher frequencies and thus provide more detailed information in the waveform, the results are more sensitive to noise and much less robust to any deviation from the assumptions about structure and source processes required. However, studies using long period instruments, such as the WWSSN long period, achieve greater stability and robustness with lower resolution. Hence, the depth determined using long period data is an average over a finite fault, and the source time function determined is relatively insensitive to high frequency information (Stein and Wiens 1986). The trade-off between the depth phases and the source time function is not serious for the small magnitude events treated in this study. The observed seismograms have, therefore, been collected from the long period WWSSN records for comparison with the synthetics.

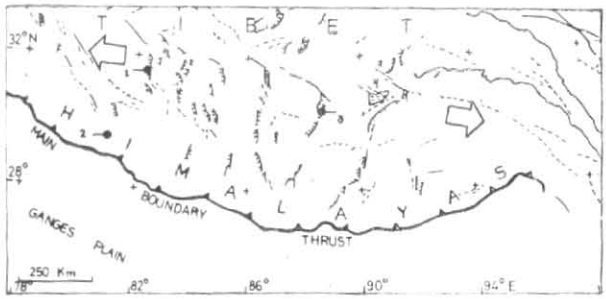

Fig. 1. Epicentral distribution of the earthquakes analysed. The numbers refer to the event number listed in Table 1. Major active normal faults of south Tibet are reproduced from Tapponnier *et al.* (1986)

In an attempt to avoid the effect of upper mantle on the synthetics generated, computations were limited to those stations whose epicentral distance lies between 30° & 90°. While the source is assumed to be a double couple point source, the far-field source time function is assumed to be trapezoidal and uniform for all stations for each event.

For shallow earthquakes with depth less than 100 km the major effects of earth structure on the *P*-wave are two pulses *pP* and *sP* due to reflections of the upgoing *P*-and *S*- waves at the earth's surface. These pulses are convolved with the instrument response of WWSSN seismographs, the far field source time function, the *Q* operator for attenuation (Carpenter 1966) in which T_P^* of one second is assumed. The source time function defined by the time constants t_0, t_1 and t_2 is obtained by the visual fit to the first half cycle of the waveform.

For each event, the focal mechanism solution has been obtained using *P*-wave first motion data and *S*-wave polarization angles read from WWSSN records. Using the mechanism solution thus obtained, the focal depth and source time function were determined by matching the waveforms. However, if the focal mechanism is not well constrained from the first motion data, a rough estimate of focal depth and source time function is first made by using stations far from the nodal planes. The nodal planes are then examined by comparing synthetics with observed seismograms at stations near the nodes to obtain optimal solutions. Using this optimal solution, the focal depths have been redetermined accurately.

3. Results

The epicentral locations of the events studied are shown in Fig. 1. To account for the unusually large thickness of the crust in the great Himalayas, the total crustal thickness used for Events 1 and 3 has been taken as 60 km as against a crustal thickness of 28 km for Event 2 whose epicentre lies very close to the main thrust axis. Table 3 lists the source parameters obtained in this study. The average focal depth with standard deviation and the source time function estimated for each event are listed in Table 4. Figs. 2-4 illustrate the fault plane solutions and comparison of synthetic and observed seismograms of the long period vertical component of *P*-waves for events listed in Table 1. In all

TABLE 3

Source parameters of the events studied

Event No.	Date	NP_1			NP_2		P-axis		T-axis	
		Strk.	Dip	Rake	Strk.	Dip	Azm.	Plg.	Azm.	Plg.
1	23 Jan 1982	203	67	—90	23	23	113	68	293	22
2	29 Jul 1980	105	64	92	290	26	197	18	10	71
3	22 Feb 1980	185	48	—72	338	46	165	77	261	2

TABLE 4

Depth and source time function for the study events

Event No.	Focal depth (km)	Std. dev. (km) and No. of stations	Source time function		
			t_0 (sec)	t_1 (sec)	t_2 (sec)
1	11	1.8 (8)	1.0	1.0	1.0
2	4	1.6 (11)	4.5	4.5	4.0
3	12	2.6 (8)	0.5	0.5	0.5

the three cases, equal-area projections of the lower hemisphere of the focal sphere are shown with solid circles as compressional and open circles as dilatational first motions. Large and small circles are long period and short period P-wave first motions respectively. Crosses are the uncertain readings and asterisks indicate nodal polarities. Arrows indicate S-wave polarization angles. Nodal lines are those listed in Table 3. The azimuth of the station, epicentral distance and the depth used for the calculation of the synthetics shown in the figures are indicated below the station code. The details of each event are described below :

Event 1 (1982 01 23 17 37 : $m_b = 6.0$)

This event had its epicentre in the southern Tibet north of the main Himalayan thrust zone. From the focal mechanism diagram shown in Fig. 2, it may be noticed that the solution requires a large dip slip component with both the nodal planes striking NNE-SSW direction. The S-wave polarization angle could be determined very accurately for two stations KEV and NUR located in the northwest quadrant of the focal sphere. Judging from the P-wave polarities and S-wave polarization angles, the strike and dip of the WNW dipping nodal plane could be well constrained. The synthetics generated by varying the rake angles were compared with the observed waveforms to get the best possible fit. The best fit requires a large component of normal faulting with the T axis trending in WNW-ESE direction. However, the strike and dip of the other nodal plane are not well constrained. Focal depths between 10 and 15 km yield best fit for as many as eight stations. The steeper nodal planes of normal faulting events may be interpreted as their fault planes because normal faults usually have planes dipping more steeply than 45° (Jaeger and Cook 1979). With this presumption, the nodal plane dipping in a WNW direction may be considered as the fault plane for this event.

Event 2 (1980 07 29 14 58 : $m_b = 6.1$)

The earthquake is located north of MBT and the solution indicates thrust faulting with the nodal planes paralleling the local structural trend. Though the nodal planes for this solution could not be determined uniquely, it is clear that the solution is dominantly a reverse fault type. The relatively small amplitude of the P-wave onset at QUE, shown by an asterisk in the mechanism diagram, indicates that the station is very close to the node. From the distribution of the first motion data it may be seen that the southward dipping nodal plane is relatively better constrained than the other nodal plane. The strike and dip of the other nodal plane are then estimated by varying the rake angle to get the best possible match between the observed and synthetic waveforms. Both the nodal planes strike parallel to the local structural trend with the P axis almost paralleling the direction of movement of Indian plate with respect to Eurasian plate. Considering the trend of tectonic features in the region and the dip angles of the nodal planes, the northerly dipping nodal plane may be interpreted as the fault plane for this event. This is because of the fact that thrusting is more probable on a shallow dipping plane than on a steeply dipping nodal plane. Fig. 3 depicts the mechanism diagram together with the synthetic and observed waveforms at eleven stations. On the basis of the best fits, it may be seen that the focal depth for this event lies between 3 and 8 km.

Event 3 (1980 02 22 03 02 : $m_b = 5.7$)

The event, with its epicentre in the southern Tibet does not yield a well constrained solution. However, the first motion data in conjunction with S-wave polarization angles could constrain well the strike and dip of the westward dipping nodal plane. The S-wave polarization angle at JER corroborates the inferred strike of the westward dipping nodal plane. By varying

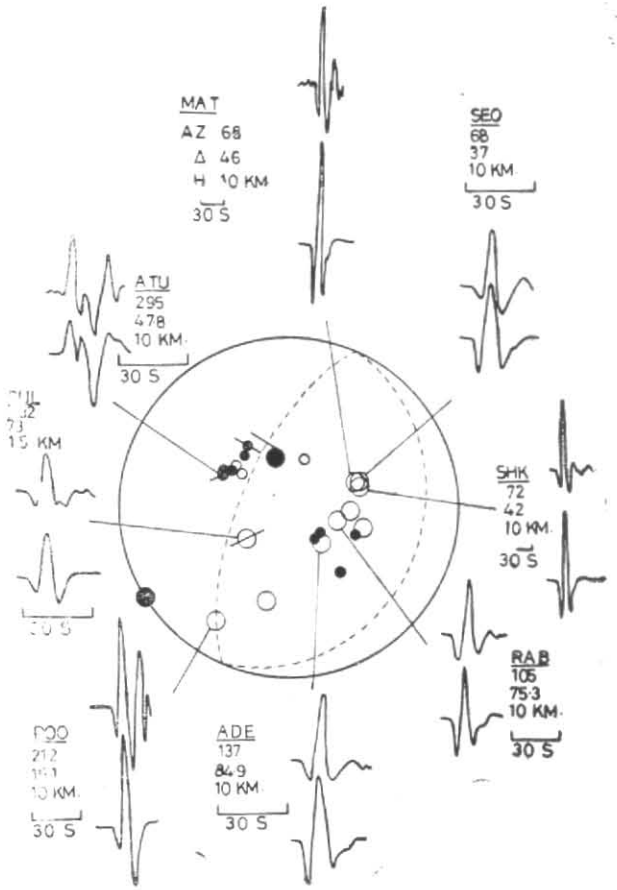

Fig. 2. A mechanism diagram and comparison of the synthetics with the observed *P*-wave records for Event 1

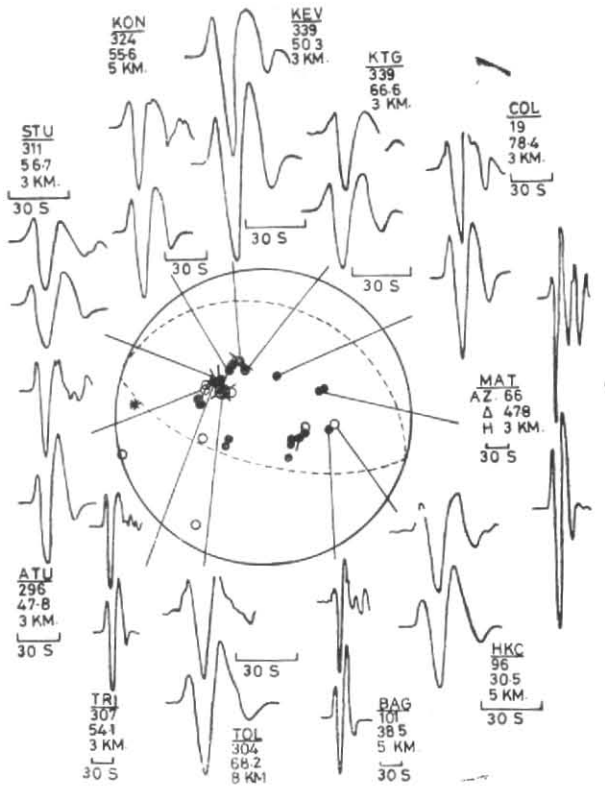

Fig. 3. A mechanism diagram and comparison of the synthetics with the observed *P*-wave records for Event 2

the rake angle, the best fit between the observed and synthetic waveforms was obtained. The fault plane solution requires a large component of normal faulting with nearly horizontal east-west trending *T* axis. The synthetics for focal depths between 10 & 15 km fit the observed records better as illustrated in Fig. 4. Considering the prominent fault traces as reported by Tapponnier *et al.* (1986), the westward dipping nodal plane may be interpreted as the fault plane for this event.

4. Discussion

The focal depths estimated from the synthetic waveform modelling for all the three study events are relatively shallower in comparison to the corresponding ISC determinations. The two methods of depth determination, ISC and the present synthetics are, however, quite different. Unlike the ISC method, the synthetic methods makes use of simultaneous matching of waveforms recorded at a number of stations round the globe with the corresponding simulated waveforms, and hence is expected to yield better estimates. How better they are, however, depends on how close is the match between them. Events 1 and 3 whose epicentres lie in southern Tibet show a large component of normal faulting with east-west trending *T* axes. For both the events, the *T* axis is more nearly horizontal than the *P* axis. As proposed by Jaeger and Cook (1979), the steeply dipping nodal planes of these normal faulting events, which dip towards west have been interpreted as their fault planes. The inferred dip directions for these events are also consistent with the prominent fault traces of Tibet reported by Tapponnier *et al.* (1986). Molnar and Chen (1983) have also obtained focal depths and fault plane solutions for 16 crustal events and two intermediate depth events beneath the highest parts of the Tibetan plateau using synthetic waveform modelling. They have observed that all the events exhibit large components of normal and strike slip faulting with east-west trending tension axes. The focal depths for all these events, including those studied in this paper, are found to be less than 15 km. The predominance of normal/strike slip faulting and the shallow focal depths of the crustal events in Tibet are attributed to crustal thinning by crustal extension. Gravitational potential energy stored in regions of high elevations, and for Tibet in the crustal root as well, would provide the energy to drive the extension and crustal thinning (Molnar and Tapponnier 1978). Thus the results of this study further corroborate the earlier inferences that the active tectonics of Tibet is predominantly controlled by extension in an east-west direction.

Event 2 with its epicentre north of MBT shows thrust faulting with the nodal planes paralleling the local structural trend. Keeping in view the Himalayan arc tectonics, the northerly dipping nodal plane with its shallow dip angle has been interpreted as the fault plane solution for this event. The *P* axis for this event shows a parallel trend with the direction of movement of Indian plate with respect to Eurasian plate (Minster and Jordan 1978 and Demets *et al.* 1990). The solution, thus, indicates crustal shortening and underthrusting of the peninsular shield mass along the Himalayan arc.

The active deformation in central Asia includes crustal shortening along the thrust faults throughout the entire Himalayan front, lateral displacement along strike slip faults, *viz.*, the Altyn Tagh and Kunlun faults in eastern and western Tibet and extension along normal faults in central Tibet (Molnar and Tapponnier 1975 and Molnar and Deng 1984). A large number of focal mechanism solutions available in literature for the main Himalayan arc (between MBF and ISZ) show thrust faulting along NW-SE oriented nodal planes. These solutions suggest that a considerable amount of energy is being released through thrust faulting along the Himalayas at present. Dattatrayam and Seno (submitted in May 1991) have studied the slip vectors of thirty nine thrust earthquakes occurring along the Himalayan thrust zone in an attempt to understand the possible relationship between the slip vectors and the velocity vectors derived from the global plate motion models of Minster and Jordan (1978) and Demets *et al.* (1990). They have also discussed the occurrence of normal and strike slip type of faulting in south Tibet in the light of a simple kinematic model which proposes that the eastern and western blocks of south Tibet are separating from each other.

Seeber *et al.* (1981) have postulated that the great Himalayan earthquakes occur south or up-dip from the Basement Thrust Front (BTF) and are interpreted as detachment events. In the interseismic periods between the great events, moderate magnitude thrust earthquakes are concentrated in the narrow belt down-dip from the BTF and the detachment appears to be aseismic. Event 2 appears to be one of those moderate size magnitude events concentrated along the narrow belt down-dip from the BTF.

The earlier inferences that the Himalaya is a zone of current thrusting limited to crustal depths (Gutenberg and Richter 1954, Fitch 1970) and that secondary structures involving normal and strike slip faulting are also present (Valdiya 1976, Banghar 1974, Chandra 1978, Molnar *et al.* 1973) are reiterated by the results of this study.

Acknowledgements

The inital work has been carried out at the International Institute of Seismology and Earthquake Engineering (IISEE), Japan, while the author was a participant of a Group Training Course on Seismology and Earthquake Engineering at the Institute during 1987-1988. The author expresses his deep sense of gratitude to the Director and staff members of IISEE, Tsukuba (Japan) for all the help extended during the tenure of the course; to Dr. Tetsuzo Seno (presently at Earthquake Research Institute, Japan) for the valuable suggestions and continued guidance in completing the study and to the Director and staff members of the ERI, University of Tokyo, Tokyo for all the help extended in obtaining copies of WWSSN seismograms.

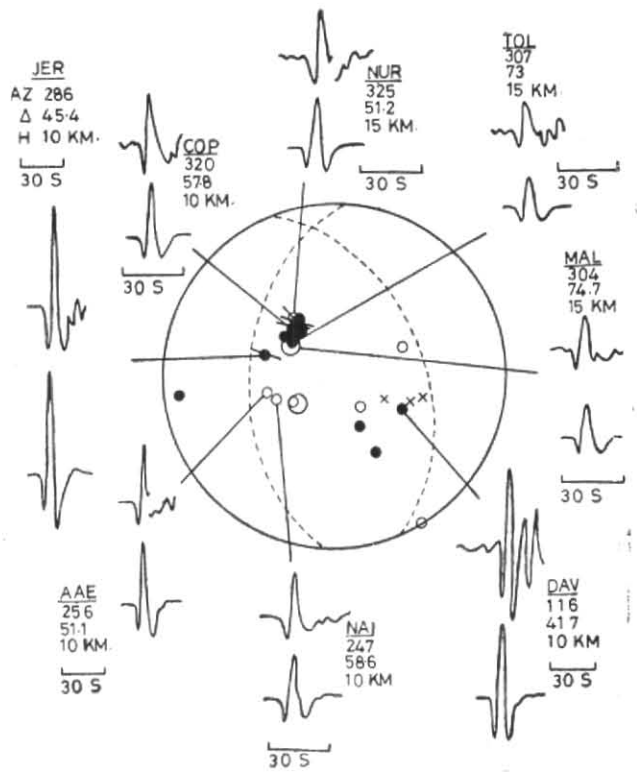

Fig. 4. A mechanism diagram and comparison of the synthetics with the observed *P*-wave records for Event 3

References

Banghar, A.R., 1974 "Focal mechanisms of earthquakes in China. Mongolia, Russia, Nepal, Pakistan and Afghanistan", *Earthquake Notes*, **45**, 1-11.

Carpenter, E.W., 1966, "Absorption of elastic waves—An operator for constant Q mechanism", Rep. 0-43166, At Weapons Res. Estab., London.

Chandra, U., 1978, "Seismicity, earthquake mechanisms and tectonics along the Himalayan mountain range and vicinity", *Phys. Earth Planet. Inter.*, **16**, 109-131.

Dattatrayam, R.S. and Seno, Tetsuzo, "Earthquake slip vectors in the Himalayan thrust zone and their tectonic implications" (To be published in *Mausam*, **44**, 1).

Demets, Charles, Richard, G. Gorden, Donald, F. Argus and Seth Stein, 1990, "Current plate motions", *Geophys. J. Int.*, **101**, 425-478.

Fitch, T.J., 1970, "Earthquake mechanisms in the Himalayan Burmese and Andaman regions and continental tectonics in central Asia", *J. Geophys. Res.*, **75**, 2699-2709.

Gutenberg, B. and Richter, C.F., 1954, *Seismicity of the Earth and associated phenomena*, Princeton Univ. Press, New Jersey, 273.

Helmberger, D.V. and Budrick, L.J., 1979, "Synthetic seismograms", *Annual review of Earth and Planetary Sciences*, **7**, 417-442.

Jaeger, J.C. and Cook, N.G.W., 1979, *Fundamentals of Rock Mechanics*, 3rd Edition Chapman & Hall, London, 593.

Kaila, K.L., Reddy, P.R. and Hatinarain, 1968, "Crustal structure in the Himalayan foothills area of north India from *P*-wave data of shallow earthquakes", *Bull. Seism. Soc. Amer.*, **58**, 597-612.

Kroeger, G.C. and Geller, R.J., 1983, "An efficient method for computing synthetic reflection seismograms for plane layered models", *EOS Trans. Amer. Geophys. Union*, **64**, 772.

Minster, J.B. and Jordan, T.H., 1978, "Present day plate motions", *J. Geophys. Res.*, **83**, 5331-5354.

Molnar, P, Fitch, T.J. and Wu., F.T., 1973, "Fault plane solutions of shallow earthquakes and contemporary tectonics in Asia", *Earth Planet. Sci. Lett.*, **19**, 101-112.

Molnar, P. and Tapponnier, P., 1975, "Cenozoic tectonics of Asia : Effects of a continental collision", *Science*, **189**, 419-426.

Molnar, P. and Tapponnier, P., 1978, "Active tectonics of Tibet", *J. Geophys. Res.*, **83**, 5361-5375.

Molnar, P. and Chen, Wang-Ping, 1983, "Focal depths and fault plane solutions of earthquakes under the Tibetan plateau", *J. Geophys. Res.*, **88**, 1180-1196.

Molnar, P. and Deng, Q., 1984, "Faulting associated with large earthquakes and the average rate of deformation in central and eastern Asia", *J. Geophys. Res.*, **89**, 6203-6227.

Seeber, L., Armbruster, J. and Quittmyer, R., 1981, "Seismicity and continental subduction in the Himalayan arc", in "Zagros, Hindukush, Himalaya Geodynamic Evolution", *Geodyn. Ser.* **3**, edited by H.K. Gupta and Delany, F.M., AGU, Wash., D.C., 215-242.

Stein, S. and Kroeger, G., 1980, "Estimating earthquake source parameters from seismological data", in Solid Earth Geophysics and Geotechnics, AMD Symp. Ser., **42**, edited by S. Nemet-Nasser, American Society of Mechanical Engineering, New York.

Stein, S. and Wiens, D., 1986, "Depth determination for shallow teleseismic earthquakes : Methods and results", *Rev. Geophys.*, **24**, 806-832.

Tapponnier, P, Peltzer, G. and Armijo, R., 1986, "On the mechanics of the collision between India and Asia", From Coward, M.P. and Ries, A.C. (eds.) Collision tectonics, Geological Society, Special Publi. No. 19, 115-157.

Valdiya, K.S., 1976, "Himalayan transverse faults and folds and their parallelism with subsurface structures of north Indian plains", *Tectonophys.*, **32**, 353-386.